

Optimization of the SNR/resolution tradeoff for registration in magnetic resonance images

S. Kale^{1,2}, J. P. Lerch¹, R. M. Henkelman^{1,2}, and X. J. Chen^{1,2}

¹Mouse Imaging Center, Toronto, Ontario, Canada, ²Medical Biophysics, University of Toronto, Toronto, Ontario, Canada

Introduction

Registration is a vital tool for medical image analysis with applications such as the evaluation of change in longitudinal studies, and building digital atlases and performing morphologic analysis. The latter have seen particularly rapid growth to study disease-specific populations and developmental biology in the brain¹. Registration has been used extensively with magnetic resonance (MR) images where imaging provides great versatility in capturing neuroanatomy. The user can acquire data as 3D volumes or 2D slices, with arbitrary resolution and orientation, while the field-of-view can be defined to fit any object. One limiting factor is the total imaging time which leaves the user with a tradeoff decision between resolution and signal-to-noise-ratio (SNR). Generally, acquisition parameters are adjusted such that the images produced satisfy human visual preferences, however, as image registration is a computer analysis task, optimization should respond to the needs of the computer analysis. This abstract presents a study investigating the optimal tradeoff between SNR and resolution in MR imaging for constant scan time to achieve optimal registration accuracy.

Methods

While images of any anatomy would suffice, images of fixed mouse neuroanatomy, acquired through a high quality microscopy protocol, were used. Fixed brain specimens, imaged in situ, were prepared similar to methods described previously². Imaging was performed on a 7 T magnet with a multichannel Varian^{INOVA} console and a three-coil probe for parallel sample imaging. Scan parameters included: a fast spin-echo pulse sequence, TR/TE = 325/8 ms, 6 echoes (fourth echo at k-space center), TE_{eff} = 32 ms, 90° flip angle, 14 mm x 14 mm x 25 mm FOV, 432 x 432 x 780 scan matrix, and 4 averages (NA). The imaging time was 11.3 hours, yielding T2-weighted images of three brains with (32 μm)³ voxels per session. Ten brains were scanned. Images had a mean SNR of 16 in homogeneous white matter. These images represented the gold standard.

Five degraded tradeoff images were simulated from each gold standard image to emulate a 1.9 h acquisition time, but at the expense of SNR or resolution or both. The first step required selecting sub-volumes of k-space from the gold standard data to represent degraded resolutions. Five sub-volumes were chosen, referred to hereafter as tradeoffs A-E, with a voxel volume step of 2x between tradeoffs (Table 1, top). The second step involved adding Gaussian-distributed random white noise to the raw data to simulate the appropriate relative NA among tradeoff data thus fixing the total effective imaging time (1.9 h). The images from each tradeoff group and the gold standard group were then independently registered, using ANIMAL^{3,4}, towards unbiased average atlases using affine and nonlinear registration⁵. Deformation fields, useful for identifying differences in morphology, were produced from the nonlinear registrations and were used to evaluate registration accuracy among the tradeoffs relative to the gold standard registration.

1.9 h time-point tradeoff images				
tradeoff	k-space volume (PE ₁ x PE ₂ x RO)	isotropic resolution (μm)	effective NA	mean SNR
A	432 x 432 x 780	32	1.0	6.4
B	344 x 344 x 620	40	1.6	11.3
C	272 x 272 x 492	51	2.5	20.2
D	216 x 216 x 390	64	4.0	35.9
E	172 x 172 x 310	81	6.3	63.0
4.8 h time-point tradeoff images				
F	432 x 432 x 780	32	1.0	10.0
G	344 x 344 x 620	40	1.6	18.3
H	272 x 272 x 492	51	2.5	32.9

The root-mean-squared error (RMSE) metric, where $RMSE^i = (\sum_N \|d^o(\mathbf{r}) - d^i(\mathbf{r})\|^2 / N)^{1/2}$, was used to quantify registration error for each tradeoff image relative to its gold standard such that $d^o(\mathbf{r})$ and $d^i(\mathbf{r})$ are the displacement vectors in the gold standard and tradeoff i , $i=A$ to E , at location \mathbf{r} , and N is the number of voxels in the brain. The entire experiment was repeated for another set of tradeoff images produced for a 4.8 h imaging time-point (F-H, Table 1, bottom) to verify that the optimal tradeoff was invariant with total imaging time.

Table 1 Data on simulated tradeoff images at 1.9 and 4.8 h fixed times.

Results and Discussion

Detailed views of the anterior commissure from tradeoffs A-E of one brain are shown in Fig. 1 illustrating the range of contrast and pixelation typical among the simulated images. Note that while tradeoff A has high resolution there is a definite loss of contrast due to noise. In contrast, tradeoff E loses resolvability while the SNR is very high. The measured SNRs of the simulated tradeoff images were within 1% of the target SNRs.

Registration succeeded in converging to an average atlas for all groups of images. Figure 2 shows a log-log plot of mean RMSE versus mean SNR across the 10 brains in each tradeoff group for the 1.9 h (●) and 4.8 h (×) sets of images, with error bars given as SEM. For the 1.9 h imaging time, tradeoff C, with SNR ~20, clearly has the minimum registration error. Tradeoff G, with SNR just below 20, presented the minimum registration error at the 4.8 h imaging time indicating that the optimal SNR is invariant.



Figure 1 A selected view of the anterior commissure among tradeoff images for one brain (1.9 h tradeoff set). The range of image quality among tradeoff images at fixed time is appreciable.

Conclusions

It has been shown that a tradeoff SNR of 20 at fixed imaging times provides appropriate images for optimal intensity-based registration. Imaging tasks that use registration for anatomical MR images should select a resolution to achieve voxel SNRs of ~20 for the best possible registration.

References

- 1 Toga AW and Thompson PM. Maps of the brain. *Anat Rec* 2001; **265**: 37-53.
- 2 Henkelman RM, et al. High throughput microimaging of the mouse brain. *Proc Intl Soc Mag Reson Med* 2006; **14**: 2010.
- 3 Collins DL, et al. Automatic 3D intersubject registration of MR volumetric data in standardized Talairach space. *J Comput Assist Tomo* 1994; **18**: 192-205.
- 4 Collins DL, et al. Automatic 3-D model-based neuroanatomical segmentation. *Hum Brain Mapp* 1995; **3**: 190-208.
- 5 Kovacevic N, et al. A three-dimensional MRI atlas of the mouse brain with estimates of the average and variability. *Cereb Cortex* 2005; **15**: 639-645.

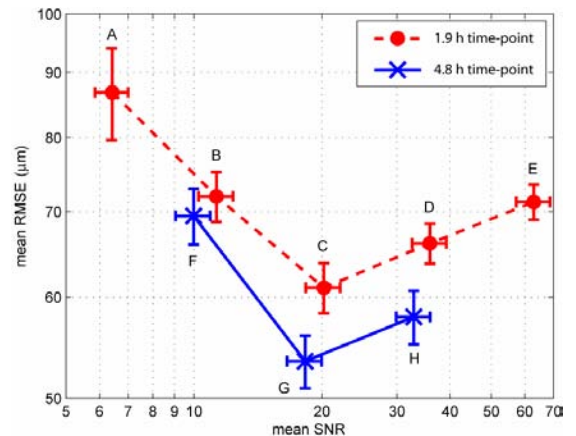


Figure 2 Plot of RMSE of tradeoff deformation fields relative to gold standard deformation fields at two imaging times.